J Eng Math (2007) 59:207–220
DOI 10.1007/s10665-007-9143-9

Interfacial hydrodynamic waves driven by chemical reactions

Antonio Pereira · Philip M. J. Trevelyan · Uwe Thiele · Serafim Kalliadasis

Received: 4 December 2006 / Accepted: 27 February 2007 / Published online: 21 April 2007

Abstract Consider the interaction between a horizontal thin liquid film and a reaction–diffusion process on the surface of the film. The reaction–diffusion process is modeled by the bistable/excitable FitzHugh–Nagumo prototype, a system of two equations for the evolution in time and space of two species, the activator and inhibitor. It is assumed that one of the species, the inhibitor, acts as a surfactant and the coupling between hydrodynamics and chemistry occurs through the solutocapillary Marangoni effect induced by spatial changes of the inhibitor's concentration. The coupled system is analyzed with a long-wave expansion of the hydrodynamic equations of motion, transport equations for the two species and wall/free-surface boundary conditions. Depending on the values of the pertinent parameters, the bistable/excitable medium can induce both periodic stationary patterns and solitary waves on the free surface.

Keywords Hydrodynamic effects induced by chemical-wave propagation · Reaction–diffusion processes · Surfactants · Thin-film flows

1 Introduction

The role of surface-tension gradients (Marangoni effect) as a cause of interfacial instabilities has been established by the pioneering studies of Pearson [1] and Sternling and Scriven [2]. Such gradients are due to either a spatially inhomogeneous temperature field (thermal Marangoni effect) or the presence of surface-active agents (surfactants) that alter the surface tension (solutal Marangoni effect).

In the context of free-surface thin liquid films, a great deal of theoretical work has been devoted to the influence of surface-tension variation on the evolution of the free surface (see [3–5] for reviews). Thermocapillarity studies include the dynamics of a liquid film flowing down a planar substrate heated either uniformly [6–12] or by a local heat source [13–15] and the evolution of an horizontal thin liquid film heated uniformly from below [16–19]. The associated problem of solutocapillarity has similarly received considerable attention. For example, De Wit et al. [20] examined in detail the stability of free thin liquid films in the presence of insoluble surfactants and long-range

A. Pereira · P. M. J. Trevelyan · S. Kalliadasis (✉)
Department of Chemical Engineering, Imperial College London, London SW7 2AZ, UK
e-mail: s.kalliadasis@imperial.ac.uk

U. Thiele
Max-Planck-Institut für Physik komplexer Systeme, D-01187, Dresden, Germany

attractive van der Waals interactions. Schwartz et al. [21] and Weidner et al. [22] investigated the role of surfactants on the leveling of thin liquid layers and correcting defects in corners, while Matar and Troian [23] scrutinized the effect of Marangoni stresses on the spontaneous spreading of insoluble surfactant monolayers on thin liquid films.

The vast majority of theoretical developments in free-surface thin-film flows has largely ignored the presence of chemical reactions that might take place within the film, on the free surface of the film or at the solid substrate. An early exception is the study by Pismen [24] who showed the formation of stationary patterns of convection and chemical activity due to a chemical reaction in a film with a free surface. The chemical system was an autocatalytic reaction for a single chemical species. We also note the study by Galez et al. [25] who provided a detailed description of the influence of a surface chemical reaction on the dynamic behavior of a thin liquid film in the presence of surface-tension gradients induced by the chemical reaction affecting insoluble surfactants. They examined the linear stability of the flat-film solution and they showed that the chemical kinetics can profoundly affect the dynamics of the film leading to oscillatory solutions absent in the pure hydrodynamic model for the free surface. They also presented numerical solutions of the free-surface evolution equation that demonstrate both oscillations and rupture.

More recently Trevelyan et al. [26] and Trevelyan and Kalliadasis [27,28] examined the evolution of a vertically falling film in the presence of a simple first-order exothermic chemical reaction. The reactive species is absorbed from the surrounding gas into the liquid where the chemical reaction takes place. The heat released/absorbed by the reaction induces a thermocapillary Marangoni effect which, in turn, affects the interface, fluid flow and absorption characteristics of the film. It was demonstrated that an exothermic reaction has a stabilizing influence on the free surface. Bifurcation diagrams for permanent solitary waves were constructed and time-dependent computations showed that the system always approaches a train of coherent structures that resemble the (infinite-domain) solitary pulses. It was further shown that the presence of chemical reactions can have a dramatic effect on the evolution of the interface and in fact can make the solitary waves dispersive. The size of dispersion was found to depend on the size of the Prandtl and Schmidt numbers while its sign could change from positive to negative leading to negative-hump solitary waves. For large dispersion and for a sufficiently large region of Reynolds numbers, the liquid layer can be excited in the form of nondissipative waves which close the criticality assume the form of Korteweg–de Vries solitons.

A related line of research studies the droplet motion caused by chemical reactions at the solid substrate underneath the droplet that produces a driving wettability gradient [29–31]. This system has been recently described by dynamical models combining a free-surface thin-film equation and a reaction–diffusion equation for the adsorbate at the substrate [32,33] (see also the simple model developed in [34]).

In this study, however, we focus on surface waves on thin films of thicknesses that are everywhere well above 100 nm and thus we exclude the problem of moving contact lines that enters the description of moving droplets. More specifically, we investigate the dynamics of an horizontal thin liquid film in the presence of insoluble reactive surfactants on the free surface of the film. This allows us to analyze the interplay between reaction, diffusion and fluid flow using a model derived with a long-wave (lubrication) approximation [4]. For the reaction–diffusion process we shall adopt the FitzHugh–Nagumo (FHN) equations [35,36] as a model system. FHN typically consists of two variables, the 'inhibitor' and the 'activator', and represents a generic model of dissipative structures in excitable and bistable media. Excitable media are non-equilibrium extended systems having a single uniform steady state that is linearly stable but susceptible to finite-size perturbations. Depending on the form of these perturbations, nonlinear wave patterns can be triggered such as solitary pulses. On the other hand, bistable systems possess two stable uniform steady states and fronts connecting the two are likely to propagate in them. Hence the FHN model has a much richer dynamics than the simple kinetic schemes employed in [25–28].

In the model presented here the FHN system induces a Marangoni flow. For simplicity we assume that this flow is due to the fact that *one* of the chemical species, the inhibitor, acts as a surfactant. The coupling between the thin-film hydrodynamics and reaction–diffusion events then occurs through the Marangoni stresses induced by the reactive surfactant. As there is no body force, hence no mean flow, any hydrodynamic flow/wave pattern on the film surface is driven purely by the reaction–diffusion events. Hence, with the exception of the vertical length scale, which evidently should be defined by the unperturbed film thickness, the characteristic length/time scales, and as a result velocity scales, for the coupled system are determined by the inhibitor. In other words, the typical length/time

scales of the interfacial waves and of the inhibitor waves are of the same order. Since thin liquid films typically evolve in slow time/space scales, both film thickness and inhibitor are 'long-wave' variables.

Hence the situation here is dramatically different to the reactive falling-film problem examined in [26–28]. Indeed in these studies, the flow is due to gravity and the dynamics is driven by the hydrodynamics with the chemical reaction playing effectively a secondary role and being 'slaved' to the hydrodynamics. While the coupling between the fluid flow and the chemical reaction is non-trivial and indeed can lead to some interesting spatio–temporal behavior, such as converting the dissipative solitary pulses on a non-reactive film to non-dissipative ones, it is the mean flow due to gravity, viscous forces and the streamwise curvature gradient which are responsible for the existence of solitary pulses on the surface of the film in the first place. It is exactly for this reason that the characteristic time, length and velocity scales in [26–28] were based on the hydrodynamics.

As mentioned earlier the interplay between hydrodynamics, reaction and diffusion is analyzed within the context of the long-wave approximation. Taking the ratio of the unperturbed film thickness to the horizontal length scale defined by the bistable/excitable medium as a small (long-wave) parameter, allows us to utilize a long-wave expansion of the reaction–diffusion–convection equations and associated free-surface boundary conditions to obtain a set of three coupled nonlinear partial differential equations for the evolution of the local film thickness and concentrations of the two species.

A linear stability analysis of these equations demonstrates that the interplay between hydrodynamics and reaction–diffusion process is not trivial. In the absence of the Marangoni effect, the free surface is linearly stable. However, it can be destabilized when it is coupled to the reaction–diffusion process and in the region where the reaction–diffusion process is linearly unstable. For the parameter values examined here, this instability leads to a spatially periodic stationary pattern on the free surface.

The remainder of our study focuses on the existence of nonlinear hydrodynamic traveling waves excited by the reaction–diffusion process. In the absence of convection there exist traveling reaction–diffusion waves which assume the form of fronts or pulses. We demonstrate that traveling waves exist also for the coupled thin-film/reaction–diffusion system. These waves take the form of fronts/pulses for the bistable/excitable medium, respectively, and pulses for the free surface. Finally, we construct bifurcation diagrams for the speed of the traveling waves as a function of the Marangoni number.

2 Problem definition

We consider a thin liquid film of viscosity μ, surface tension σ and density ρ on an horizontal planar substrate. We restrict ourselves to the one-dimensional problem. A Cartesian coordinate system (x, y) is chosen so that x is in the direction parallel to the substrate and y is the outward-pointing coordinate normal to the substrate. The substrate is then located at $y = 0$ while $y = h(x, t)$ denotes the location of the interface. The governing bulk equations are conservation of mass and the Navier–Stokes equations of motion,

$$u_x + v_y = 0 \tag{1a}$$

$$u_t + uu_x + vu_y = -\frac{1}{\rho}p_x + \nu(u_{xx} + u_{yy}) \tag{1b}$$

$$v_t + uv_x + vv_y = -\frac{1}{\rho}p_y + \nu(v_{xx} + v_{yy}) - g, \tag{1c}$$

where u and v are the horizontal and vertical components of the velocity field, respectively, and p is the liquid pressure. g is the gravitational acceleration and $\nu = \mu/\rho$ is the kinematic viscosity.

On the wall we have the usual no-slip/no-penetration boundary condition,

$$u = v = 0, \quad \text{on} \quad y = 0, \tag{2}$$

and on the interface $y = h(x, t)$ the kinematic boundary condition and the normal and tangential stress balances,

$$v = h_t + uh_x \tag{3a}$$

$$\frac{1}{\rho}(p-p_0)+\frac{2\nu}{1+h_x^2}\left[-(h_x^2u_x+v_y)+h_x(u_y+v_x)\right]=-\frac{\sigma}{\rho}\frac{h_{xx}}{(1+h_x^2)^{3/2}} \tag{3b}$$

$$-2\nu h_x(u_x-v_y)+\nu(1-h_x^2)(u_y+v_x)=(1+h_x^2)\frac{1}{\rho}\left(\frac{\mathrm{d}\sigma}{\mathrm{d}s}\right), \tag{3c}$$

where s is an arclength coordinate along the interface and p_0 is the pressure of the ambient gas phase above the liquid film. The surface-tension gradient in (3c) is due to the presence of insoluble surfactants on the interface. These surfactants are involved in a reaction–diffusion process. Notice that, as is typically the case with the Marangoni effect, we assume that the variation of surface tension will not influence the normal stresses on the interface; the surface-tension gradient, however, will create a finite tangential stress at the interface.

As a model system for the reaction–diffusion process we adopt the FHN equations discussed in Sect.1. In the absence of fluid flow, the FHN transport equations are written in the following dimensional form,

$$\zeta_t=D_{s\zeta}\zeta_{xx}+k_\zeta(\zeta-b_2'\zeta^3-b_1'\xi), \tag{4a}$$

$$\xi_t=D_{s\xi}\xi_{xx}+k_\xi(\zeta-a_1'\xi-a_0'), \tag{4b}$$

which is a system of two partial-differential equations for the evolution in time and space of two variables: ζ, referred to as the 'activator', and ξ, referred to as the 'inhibitor'. The accumulation of ζ, ξ is due to two effects: molecular diffusion in the streamwise direction and generation/consumption by the chemical reaction (first and second terms in the right-hand side of Eqs. 4a, b, respectively). In the absence of diffusion, increasing ζ increases the accumulation of both ξ and ζ while increasing ξ lowers them, hence the terms 'activator/inhibitor'. For excitable media the ratio k_ζ/k_ξ is large [35] and ζ, ξ are also referred to as 'fast, slow variables', respectively. The FHN system in (4) is parameterized by eight parameters: the surface-diffusion coefficients $D_{s\zeta}$ and $D_{s\xi}$, the reaction-rate constants k_ζ and k_ξ and the kinetic parameters a_0', a_1', b_1' and b_2'. With the exception of a_0', all these parameters are positive [36].

Let us now include the effect of convection on the FHN model in (4). The two species are assumed to be insoluble, i.e., they remain on the interface and do not diffuse into the bulk. The derivation of the basic convective–diffusion equation that governs the transport of a non-reactive insoluble species along a deforming interface is given e.g. in [37,38]. Note that the FHN model is actually obtained after a lengthy reduction process of a rather complex initial set of equations [39]. Accordingly, ζ and ξ represent combinations of concentrations of the original high-dimensional model and only remotely correspond to the initial physical variables. As a consequence, Eqs. 4a, b admit negative values for ζ and ξ. Notice, for instance, the symmetry $(\zeta, \xi) \to (-\zeta, -\xi)$, if $a_0' = 0$.

Nevertheless, we can assume that we have two actual chemical species: imagine a physical experiment that records the variation of two concentrations Ξ and Z at steady state and in the absence of diffusion. One set of steady states is found to be described by the equation $Z-\zeta_\mathrm{m}'-b_2'(Z-\zeta_\mathrm{m}')^3-b_1'(\Xi-\xi_\mathrm{m}')=0$ which has an inflection point at $(\zeta_\mathrm{m}', \xi_\mathrm{m}')$ in the (Z, Ξ)-plane. The quantities ζ_m' and ξ_m' are defined by the chemical system. The transformation $\zeta = Z-\zeta_\mathrm{m}'$ and $\xi = \Xi-\xi_\mathrm{m}'$ then shifts the inflection point to the origin of the (ζ, ξ)-plane. In this plane the steady states are given by $\zeta-b_2'\zeta^3-b_1'\xi=0$ which is the same with setting the right-hand side of Eq. 4a equal to zero (in the absence of diffusion). ζ and ξ now represent deviations from ζ_m' and ξ_m' while $Z=\zeta+\zeta_\mathrm{m}'$ and $\Xi=\xi+\xi_\mathrm{m}'$ are always positive since they correspond to concentrations of actual chemical species (obviously the steady-states curve in the (Z, Ξ)-plane should not cross the $Z=\Xi=0$ axes). Ensuring positivity for Z and Ξ is essential if these variables are to describe species transported by the flow.

The transport equations in the presence of convection for the two species overall concentration, $\zeta_\mathrm{m}'+\zeta$ and $\xi_\mathrm{m}'+\xi$, can then be obtained by a straightforward extension of the convection–diffusion equation given in [37,38] to account for the presence of a chemical reaction which simply adds to the right-hand sides of the equations the

source terms due to the chemical reaction:

$$\zeta_t + u\zeta_x + \frac{\zeta'_{\rm m} + \zeta}{1 + h_x^2}\left[(u_x + h_x v_x) + h_x(u_y + h_x v_y)\right] = D_{s\zeta}\frac{1}{\sqrt{1 + h_x^2}}\left(\frac{\zeta_x}{\sqrt{1 + h_x^2}}\right)_x + k_\zeta(\zeta - b'_2\zeta^3 - b'_1\xi), \tag{5a}$$

$$\xi_t + u\xi_x + \frac{\xi'_{\rm m} + \xi}{1 + h_x^2}\left[(u_x + h_x v_x) + h_x(u_y + h_x v_y)\right] = D_{s\xi}\frac{1}{\sqrt{1 + h_x^2}}\left(\frac{\xi_x}{\sqrt{1 + h_x^2}}\right)_x + k_\xi(\zeta - a'_1\xi - a'_0). \tag{5b}$$

The first two terms in the left-hand sides of these reaction–diffusion–convection equations account for the material time derivative of the concentration fields relative to the flow and the third term is due to the stretching of the interface. The first terms in the right-hand sides originate from the molecular diffusion terms of the FHN model in (4) appropriately modified to account for diffusive motion along a deformable interface and the last terms are simply source contributions originating from the kinetic terms of the FHN model in (4). Setting $\zeta'_{\rm m} = \xi'_{\rm m} = 0$ in (5) corresponds to the case of ζ, ξ being reduced variables representing combinations of concentrations of a higher-dimensional model and not actual chemical species, as discussed earlier.

The interaction between the fluid flow and the excitable medium takes place in two ways. On the one hand, the flow changes the distribution of the species at the film surface by convection. On the other hand, the excitable medium acts upon the surface through the surface tension. The system is hence closed with a constitutive equation that expresses the variation of surface tension as a function of the species concentration. We assume that only one of the two species, the inhibitor, acts as a surfactant and alters the surface tension. This allows a substantial simplification of the problem. The solutocapillarity effect is modeled by using a linear approximation for the surface tension as a function of surfactant concentration,

$$\sigma(\xi'_{\rm m} + \xi) = \sigma_0 - \gamma\xi \tag{6}$$

where $\sigma_0 = \sigma(\xi'_{\rm m})$ and $\gamma > 0$ for typical liquids.

3 Scalings and dimensionless equations

The vertical lengthscale h^* is determined by the hydrodynamics. Hence, if h_0 denotes the flat-film thickness, then $h^* = h_0$. On the other hand, the horizontal length scale ℓ^* is set by the reaction–diffusion process that drives the hydrodynamics, more specifically the inhibitor ξ which after all is the variable that affects the hydrodynamics through the Marangoni effect. Similarly, the characteristic velocity u^* in the horizontal direction is also defined by ξ. Hence, the characteristic time scale is taken as ℓ^*/u^*. We then introduce the non-dimensionalization

$$x \to h^* x/\eta, \quad y \to h^* y, \quad t \to \ell^* t/u^*, \tag{7a}$$

$$u \to u^* u, \quad v \to \eta u^* v, \quad h \to h^* h, \quad p \to p_0 + (\rho\nu u^*\ell^*/h^{*2})p, \tag{7b}$$

$$\zeta \to \zeta^*\zeta, \quad \xi \to \xi^*\xi. \tag{7c}$$

where

$$\eta = h^*/\ell^* \tag{7d}$$

is the ratio of vertical and lateral length scales and the characteristic scales are given by

$$u^* = \sqrt{D_{s\xi}k_\xi\zeta^*/\xi^*}, \quad \zeta^* = 1/\sqrt{b'_2}, \quad \xi^* = \zeta^*/b'_1, \tag{8a}$$

$$\ell^* = \sqrt{(D_{s\xi}\xi^*)/(k_\xi \zeta^*)}, \quad h^* = h_0. \tag{8b}$$

In terms of the above non-dimensional variables, the equations of motion and continuity equation (1) become,

$$u_x + v_y = 0, \tag{9a}$$

$$\eta \mathrm{Re}(u_t + uu_x + vu_y) = -p_x + \eta^2 u_{xx} + u_{yy}, \tag{9b}$$

$$\eta^3 \mathrm{Re}(v_t + uv_x + vv_y) = -p_y + \eta^4 v_{xx} + \eta^2 v_{yy} - \mathrm{Bo}, \tag{9c}$$

subject to the wall boundary conditions,

$$u = v = 0 \quad \text{on} \quad y = 0, \tag{10}$$

and the dimensionless versions of the interfacial boundary conditions in (3):

$$v = h_t + uh_x, \tag{11a}$$

$$p + \frac{2\eta^2}{1+\eta^2 h_x^2}\left[(1-\eta^2 h_x^2)u_x + h_x(u_y + \eta^2 v_x)\right] = -(\mathrm{We} - \eta^2 \mathrm{Ma}\xi)\frac{h_{xx}}{(1+\eta^2 h_x^2)^{3/2}}, \tag{11b}$$

$$-4\eta^2 h_x u_x + (1-\eta^2 h_x^2)(u_y + \eta^2 v_x) = -\sqrt{1+\eta^2 h_x^2}\,\mathrm{Ma}\,\xi_x. \tag{11c}$$

On the interface we also have the dimensionless versions of the transport equations for the species ξ, ζ in (5):

$$\begin{aligned}\zeta_t + u\zeta_x + \frac{\zeta_\mathrm{m} + \zeta}{1+\eta^2 h_x^2}\left[(u_x + \eta^2 h_x v_x) + h_x(u_y + \eta^2 h_x v_y)\right] \\ = \frac{1}{\delta}\left(\frac{\zeta_{xx}}{1+\eta^2 h_x^2} - \frac{\eta^2 \zeta_x h_x h_{xx}}{(1+\eta^2 h_x^2)^2}\right) + K(\zeta - \zeta^3 - \xi),\end{aligned} \tag{12a}$$

$$\begin{aligned}\xi_t + u\xi_x + \frac{\xi_\mathrm{m} + \xi}{1+\eta^2 h_x^2}\left[(u_x + \eta^2 h_x v_x) + h_x(u_y + \eta^2 h_x v_y)\right] \\ = \frac{\xi_{xx}}{1+\eta^2 h_x^2} - \frac{\eta^2 \xi_x h_x h_{xx}}{(1+\eta^2 h_x^2)^2} + (\zeta - a_1\xi - a_0).\end{aligned} \tag{12b}$$

The governing dimensionless parameters are,

$$\mathrm{Re} = \frac{u^* h^*}{\nu}, \quad \mathrm{Bo} = \eta\frac{g h^{*2}}{\nu u^*}, \quad \mathrm{We} = \eta^3\frac{\sigma_\mathrm{m}}{\rho \nu u^*}, \quad \mathrm{Ma} = \eta\frac{\gamma \xi^*}{\rho \nu u^*}, \tag{13a}$$

$$\delta = \frac{D_{s\xi}}{D_{s\zeta}}, \quad K = \frac{\xi^*}{\zeta^*}\frac{k_\zeta}{k_\xi}, \quad \zeta_\mathrm{m} = \frac{\zeta'_\mathrm{m}}{\zeta^*}, \quad \xi_\mathrm{m} = \frac{\xi'_\mathrm{m}}{\xi^*}, \quad a_0 = \frac{a'_0}{\zeta^*}, \quad a_1 = a'_1\frac{\xi^*}{\zeta^*}, \tag{13b}$$

with Re the Reynolds number, Bo the Bond number, We the Weber number and Ma the Marangoni number. The remaining six parameters in (13b) are related to the excitable medium only.

Equations 11c and 12 show that the coupled hydrodynamic-FHN system has a feedback mechanism. The key for this mechanism is convection: ξ affects the hydrodynamics through the Marangoni term in the tangential stress balance and the hydrodynamics in turn changes both ξ and ζ through convection in the left-hand sides of the transport equations (12).

4 Long-wave equations

The complexity of the free-boundary problem developed in the preceding section for the evolution of a thin film coupled to the FHN model can be removed by invoking a long-wave analysis of the equations of motion and associated wall/free-surface boundary conditions. A detailed review of the long-wave approximation in the absence of chemical reactions is given by Oron et al. [4]. The basic assumption is that the ratio η of the mean film thickness ($\sim h_0$) to the characteristic wavelength of any waves on the free surface is small. This allows an asymptotic reduction of the governing equations and associated boundary conditions to a single highly nonlinear partial differential equation of the evolution type formulated in terms of the local film thickness h. For surfactant-driven thin film flows the free-surface evolution equation has been derived in [38,40,41].

The basic assumption here is that both ξ and h are long-wave variables. We outline the main steps of the long-wave expansion. We assume that Bo, We and Ma are at most of $O(1)$ with respect to η. Re is also assumed to be at most of $O(1)$ (lubrication approximation). The relative order of magnitude between δ, K and η need not be specified. The pressure field and streamwise velocity field at $O(1)$ are found to be,

$$p = \mathrm{Bo}(h - y) - \mathrm{We}h_{xx}, \tag{14}$$

$$u = (\mathrm{Bo}h - \mathrm{We}h_{xx})_x \, y(y - 2h)/2 - \mathrm{Ma}\xi_x y, \tag{15}$$

respectively, and the Reynolds number does not appear at this level of approximation. The v-velocity is then easily obtained from (9a) and (10). Substituting u and v in the kinematic boundary condition (11a) and u into the leading-order versions of the transport equations (12) then yields a set of three partial differential equations for the evolution in time and space of the three surface fields h, ζ, and ξ:

$$h_t = \left(\frac{1}{3}\mathrm{Bo}h^3 h_x - \frac{1}{3}\mathrm{We}h^3 h_{xxx} + \frac{1}{2}\mathrm{Ma}h^2\xi_x\right)_x, \tag{16a}$$

$$\zeta_t = \left(\frac{1}{2}\mathrm{Bo}h^2(\zeta_\mathrm{m} + \zeta)h_x - \frac{1}{2}\mathrm{We}h^2(\zeta_\mathrm{m} + \zeta)h_{xxx} + \mathrm{Ma}h(\zeta_\mathrm{m} + \zeta)\xi_x\right)_x + \frac{1}{\delta}\zeta_{xx} + K(\zeta - \zeta^3 - \xi), \tag{16b}$$

$$\xi_t = \left(\frac{1}{2}\mathrm{Bo}h^2(\xi_\mathrm{m} + \xi)h_x - \frac{1}{2}\mathrm{We}h^2(\xi_\mathrm{m} + \xi)h_{xxx} + \mathrm{Ma}h(\xi_\mathrm{m} + \xi)\xi_x\right)_x + \xi_{xx} + \zeta - a_1\xi - a_0. \tag{16c}$$

This system shows the couplings between the three variables h, ζ and ξ. These couplings are due to the Marangoni effect and convection: h affects both ζ and ξ through the convective flow terms in the right-hand sides of the reaction–diffusion–convection equations (16b, c). Note that, even for a non-deformable interface, i.e., $h = 1$, there is still a convective flow in Eqs. 16b, c due to the Marangoni effect that induces an interfacial velocity, $-\mathrm{Ma}\xi_x h$, in this case (Eq. 15). ζ and ξ are of course coupled to each other through the FHN kinetic terms while ξ affects h through the Marangoni term in (16a) (the coupling between h and ζ is indirect through ξ).

5 Linear stability analysis

We now consider the linear stability of the trivial solution $[h, \zeta, \xi] = [1, \zeta_0, \xi_0]$ where ζ_0 and ξ_0 are given from

$$\zeta_0 - \zeta_0^3 - \xi_0 = 0, \tag{17a}$$

$$\zeta_0 - a_1\xi_0 - a_0 = 0. \tag{17b}$$

In the (ζ_0, ξ_0)-plane (17a) forms an S-type curve and (17b) a straight line. Depending on the values of a_0 and a_1, there may be one to three intersections between the two curves corresponding to one to three spatially uniform steady states, a well known result for the FHN model [36].

Linearizing Eq. 16 about the chosen steady state and substituting the usual normal mode $\sim \exp\{\lambda t + \mathrm{i}kx\}$ in the linearized equations, yields the dispersion relationship

$$\lambda^3 + P\lambda^2 + Q\lambda + R = 0 \tag{18}$$

for the complex growth rate λ as a function of wavenumber k, with

$$P = K\beta + \frac{k^2}{\delta} + (M+1)k^2 + a_1 + \frac{k^2}{3}(\mathrm{Bo} + \mathrm{We}k^2), \tag{19a}$$

$$Q = \left(K\beta + \frac{k^2}{\delta}\right)\left[(M+1)k^2 + a_1\right] + K + \alpha M k^2 + \frac{k^2}{3}(\mathrm{Bo} + \mathrm{We}k^2)\left[K\beta + \left(\frac{1}{\delta} + \frac{M}{4} + 1\right)k^2 + a_1\right], \tag{19b}$$

$$R = \frac{k^2}{3}(\mathrm{Bo} + \mathrm{We}k^2)\left\{\left(K\beta + \frac{k^2}{\delta}\right)\left[\left(\frac{M}{4} + 1\right)k^2 + a_1\right] + K + \frac{1}{4}\alpha M k^2\right\}, \tag{19c}$$

where

$$\alpha = \frac{\zeta_\mathrm{m} + \zeta_0}{\xi_\mathrm{m} + \xi_0}, \quad \beta = 3\zeta_0^2 - 1, \quad \text{and} \quad M = (\xi_\mathrm{m} + \xi_0)\mathrm{Ma}. \tag{19d}$$

If all parameters in (19a–d) are strictly positive, $P > 0$, $Q > 0$ and $PQ > R$. According to the Routh–Hurwitz criterion then, the real parts of all three roots of (18) are strictly negative and the corresponding uniform steady state is linearly stable. The reactive surfactants then act in a similar fashion to non-reactive ones: a classical linear stability analysis of an horizontal thin film in the presence of (non-reactive) surfactants shows that surfactants have a stabilizing influence on the film [42]. In this case $\mathrm{Ma} > 0$. A destabilization of the whole system can then occur if $\mathrm{Ma} < 0$, i.e., $\gamma < 0$ or the values of ζ_m and ξ_m are such that α and/or M are negative (indeed although surface tension typically decreases with concentration there are special systems which are known to display the opposite behavior).

Another possibility that we will examine in detail here is the case $\beta < 0$. Since β is merely the opposite of the derivative of the function $\xi_0(\zeta_0)$ given by Eq. 17a, the steady state in this case is located on the inner branch of the S-type curve defined by Eq. 17a. Let us set $a_0 = 0$ and focus on the state $h = 1$, $\zeta_0 = 0$ and $\xi_0 = 0$ which is always a spatially uniform steady solution of the system independently of the value of a_1. In that case, $\beta = -1$. When $\mathrm{Ma} = 0$, the hydrodynamic system is decoupled from the FHN equations and the equation for the dispersion relationship in (18) can be factorized:

$$\left[\lambda + \frac{k^2}{3}(\mathrm{Bo} + \mathrm{We}k^2)\right]\left[\lambda^2 + \left(K\beta + \frac{k^2}{\delta} + k^2 + a_1\right)\lambda + \left(K\beta + \frac{k^2}{\delta}\right)(k^2 + a_1) + K\right] = 0, \tag{20}$$

where the first factor corresponds to h and the second factor accounts for the chemical system. The solid lines in Fig. 1 show λ as a function of k—for the parameter values chosen λ is real. One of the roots (marked as 1) corresponds to h and two of the roots correspond to the chemical system (marked as 2 and 3). The thin film is linearly stable while the chemical system is linearly unstable as can be deduced directly from Eq. 20. The two reaction–diffusion modes (curves (2a) and (3a) in the figure) exhibit a strictly positive growth rate for $k = 0$. Furthermore, the phase velocities for all modes vanish.

Increasing now the Marangoni number to 8 will change the location of the dispersion curves with the exception of curve (3a) which only moves slightly so that (3b) is effectively on top of (3a). The new set of curves shown with the dashed lines in Fig. 1 is qualitatively similar to that obtained for $\mathrm{Ma} = 0$: in all cases we have one linearly stable mode and two linearly unstable modes with a finite band of unstable modes extending from $k = 0$ up to a critical wavenumber above which they are stable, and the growth rate for $k = 0$ remains unaltered. The Marangoni effect shrinks the range of unstable modes for dispersion curve (2). It has a small influence, however, on the stability characteristics of the remaining two curves.

Since all three variables are coupled for $\mathrm{Ma} \neq 0$, the two unstable growth rate curves in Fig. 1 lead to an instability for all three variables. Hence, despite the fact that the free surface is linearly stable for $\mathrm{Ma} = 0$, its coupling to the linearly unstable reaction–diffusion system through the Marangoni effect leads to its destabilization. Figure 2 shows

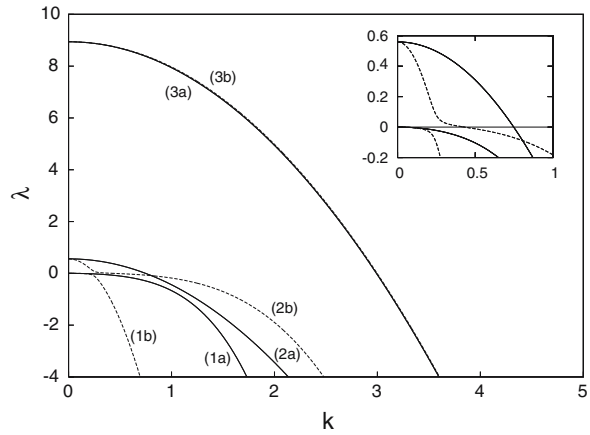

Fig. 1 Dispersion curves for $K = 10$, $\delta = 1$, $\zeta_m = 1$, $\xi_m = 1$, $a_0 = 0$, $a_1 = 0.5$, $\mathrm{Bo} = 1$, and $\mathrm{We} = 1$. Two different values of the Marangoni number have been used: $\mathrm{Ma} = 0$ ((1,2,3a)-solid lines) and $\mathrm{Ma} = 8$ ((1,2,3b)-dashed lines). Inset: enlarged view of the dispersion curves close to $\lambda = 0$. As the Marangoni number increases, the range of unstable modes decreases

the development of a spatially periodic steady state for the free surface. The pattern emerges from the flat film for $\mathrm{Ma} = 0$ and grows as Ma increases. The profiles for the three fields have been constructed numerically using the continuation software AUTO97 [43]. This stationary spatially periodic state might be unstable in time-dependent computations and hence we refrain from calling it a 'Turing pattern'. Such computations are beyond the scope of the present study.

Interestingly, although ξ diminishes as Ma increases, h which is coupled to ξ through the Marangoni effect, is amplified. This is because the maximum value of $|\mathrm{Ma}\xi_x|$ in the domain increases as Fig. 2c indicates. Indeed, it is $\mathrm{Ma}\xi_x$ that affects the evolution of the free surface (see (16)) and clearly the Marangoni effect has the maximum possible influence when $|\mathrm{Ma}\xi_x|$ is maximum.

Note that ξ has a local minimum and maximum corresponding to a local maximum/minimum, respectively, for the surface tension. This then triggers an interfacial tangential stress from the right to the left thus causing convective flow and free-surface deformation. This flow is in turn causing a convective transport of surfactants from the right to the left reducing the concentration of the surfactants. As we pointed out earlier the coupled thin film-FHN system has a feedback mechanism driven by convection: for the situation depicted in Fig. 2, ξ causes the flow and the flow homogenizes ξ.

6 Hydrodynamic traveling waves driven by FHN traveling waves

We now seek traveling wave solutions propagating at a constant speed c. Transforming Eq. 16 to a frame moving with speed c, $z = x - ct$ and $\partial/\partial t = -c\partial/\partial z$, converts (16) to a set of ordinary differential equations parameterized by c. This is effectively a nonlinear eigenvalue problem for c and can be written as an 8th-order dynamical system.

Although the spatially uniform steady states located in the outer branches of the S-type curve of Eq. 17a in the (ζ, ξ)-plane (i.e., $\beta > 0$) are linearly stable when $M > 0$ and $\alpha > 0$, there still exist traveling waves connecting these states [35,36]. Such waves typically assume the form of fronts or pulses, depending on the values of the reaction–diffusion parameters and they have been analyzed using elements from dynamical systems theory, e.g., a pulse corresponds to a homoclinic orbit connecting a stable fixed point (of the saddle node type) of the associated dynamical system.

Such reaction–diffusion fronts/pulses can also excite hydrodynamic traveling waves through finite-amplitude bifurcations even though the coupled thin-film/reaction–diffusion system might be linearly stable. Such finite-amplitude bifurcations lead to pulses on the surface of the film (homoclinic bifurcations). A detailed analysis of these waves using elements from dynamical systems theory is beyond the scope of the present study.

Typical free-surface waves with solitonic features are shown in Figs. 3 and 5, excited by fronts and pulses, respectively, of the bistable/excitable medium. These solutions have been constructed numerically using also the

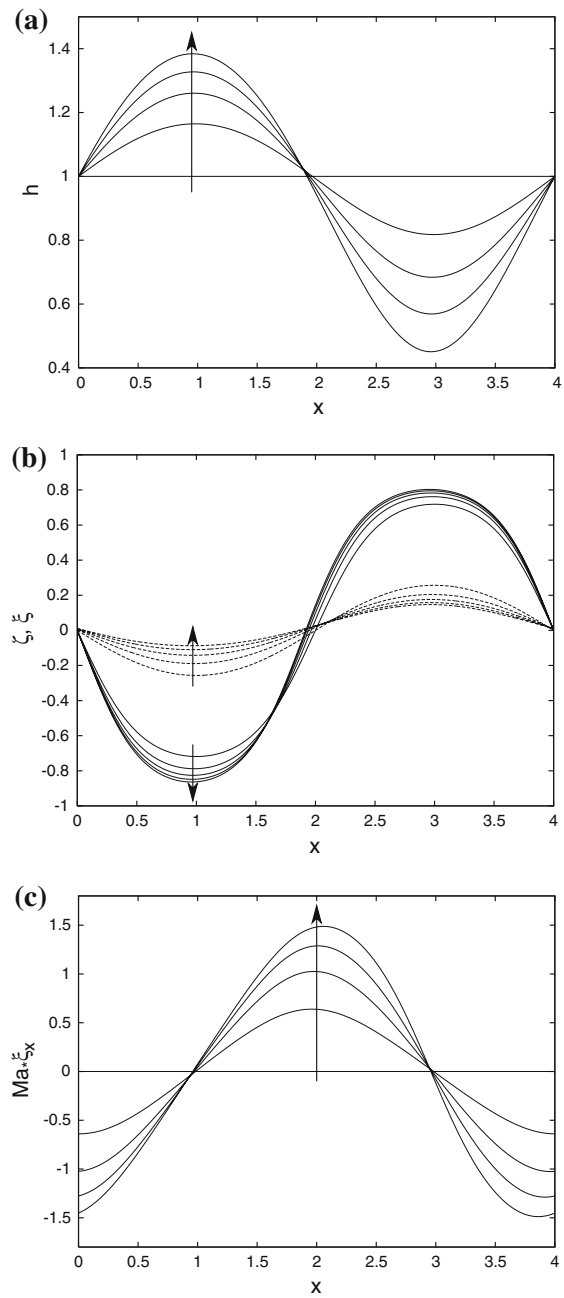

Fig. 2 Spatially periodic stationary pattern over one period; (**a**) free-surface profile for different values of the Marangoni number: Ma = 0, 2, 4, 6 and 8. The values of the remaining parameters are given in Fig. 1; (**b**) corresponding profiles of ζ (solid lines) and ξ (dashed lines); (**c**) corresponding profile for $\mathrm{Ma}\xi_x$. The arrows point to the direction of increasing Ma

continuation software AUTO97 [43]. Interestingly the shape of the free-surface solitary waves is similar to that obtained in falling liquid films [8,10,11] and consists of a primary solitary hump preceded by a series of small bow waves at the front (for large values of Ma the bow waves are very small compared to the primary hump).

In the front regime, increasing the Marangoni number amplifies the maximum amplitude of the free-surface solitary waves. This results in a smoother front for the bistable medium with the exception of the activator that develops a pronounced dimple at the front. Figure 4 shows the bifurcation diagram for the velocity c as a function of Ma in the front case. Notice that the interplay between the flow and the bistable medium leads to an initial deceleration of the waves followed by acceleration as Ma increases further.

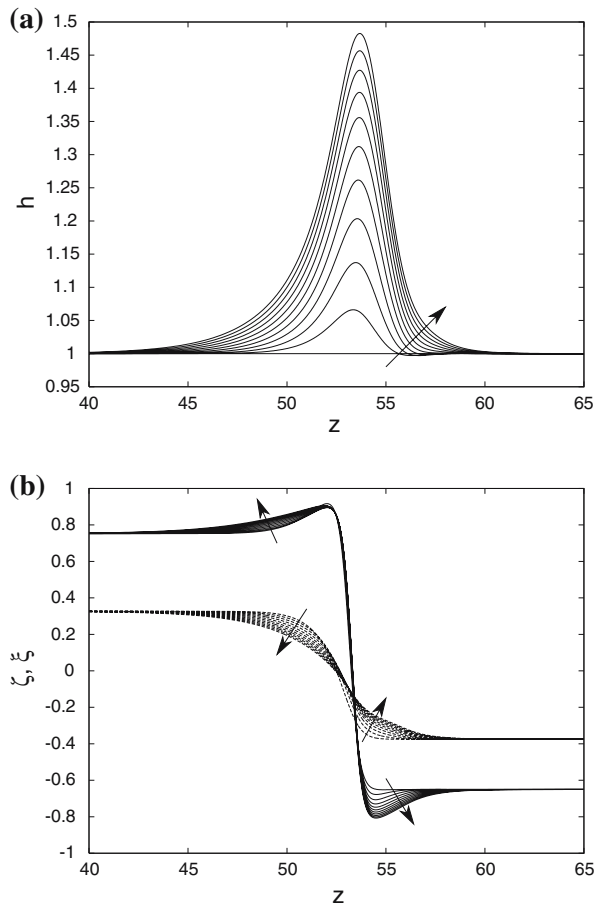

Fig. 3 Traveling waves of the coupled thin film-FHN system for $K = 10$, $\delta = 1$, $\zeta_m = 1$, $\xi_m = 1$, $a_0 = 0.1$, $a_1 = 2.0$, Bo $= 1$ and We $= 1$; (**a**) Free-surface solitary waves excited by FHN fronts for Ma $= 0-10$ in steps of 1. The arrows point in the direction of increasing Ma; (**b**) corresponding reaction–diffusion fronts for ζ (solid lines) and ξ (dashed lines)

In the pulse regime, increasing the Marangoni number again amplifies the maximum amplitude of the solitary waves and results in a smoother wave for the excitable medium with the exception of the activator whose depression at the back of the primary pulse deepens slowly as it moves to the left. Figure 6 depicts the corresponding bifurcation diagram for the velocity c as a function of Ma. Now the velocity is a monotonically increasing function of Ma while for the parameter values examined here pulses travel faster than fronts.

7 Conclusions

The coupling between bistability/excitability and diffusion can lead to a wide range of wave-propagation phenomena such as traveling fronts and pulses. Not surprisingly, therefore, bistable/excitable media have been used frequently as model systems in a wide variety of chemical and biological problems. Here we analyzed the interaction between an horizontal thin liquid film and a bistable/excitable medium on the surface of the film. The thin film and the bistable/excitable medium were coupled through a solutal Marangoni effect induced by one of the two chemical species, the inhibitor.

By utilizing a long-wave approximation of the equations of motion, transport equations of the two species and associated wall/free-surface boundary conditions, we obtained a set of three coupled nonlinear partial differential equations for the evolution in time and space of the free surface and the concentrations of the two species. These equations account for the Marangoni effect as well as the effect of convection on the reaction–diffusion process.

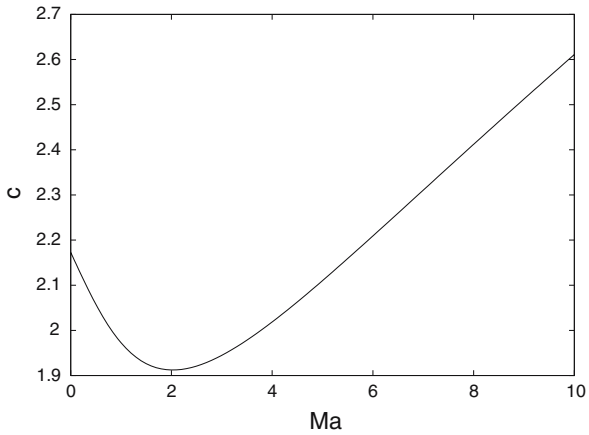

Fig. 4 Bifurcation diagram in the front case for the velocity c of the traveling waves as a function of the Marangoni number Ma and for the parameter values in Fig. 3. The coupling of the free surface and the bistable medium leads to slower waves for small Ma and faster waves for large Ma

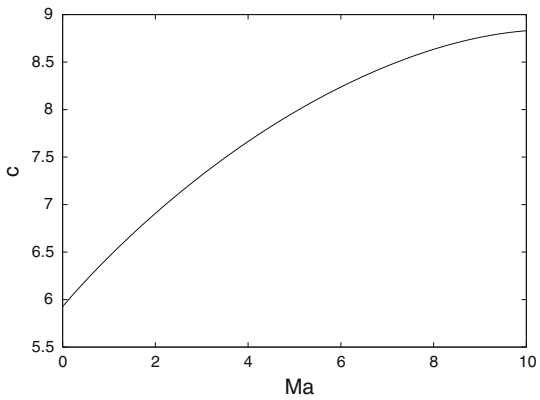

Fig. 6 Bifurcation diagram in the pulse case for the velocity c of the traveling waves as a function of the Marangoni number Ma and for the parameter values in Fig. 5. The coupling of the free surface and the excitable medium leads to faster waves

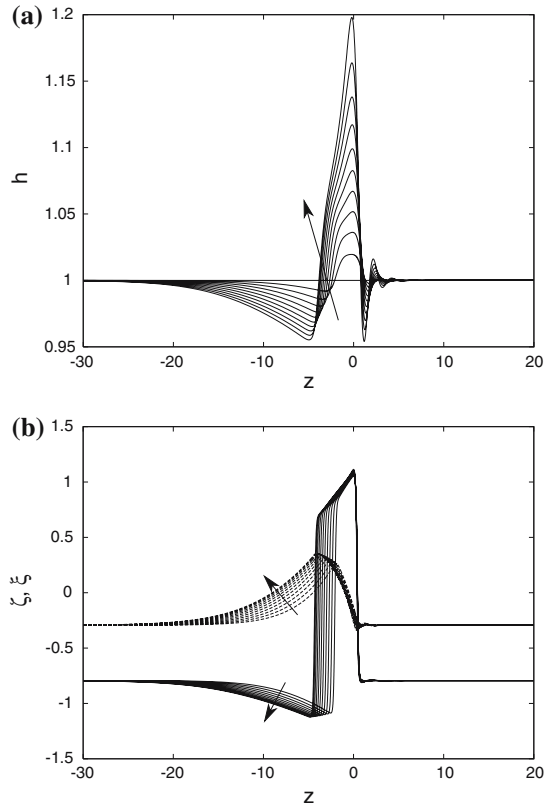

Fig. 5 Traveling waves of the coupled thin film-FHN system for $K = 100$, $\delta = 1$, $\zeta_m = 0$, $\xi_m = 0$, $a_0 = -0.5$, $a_1 = 1.0$, $\mathrm{Bo} = 1$ and $\mathrm{We} = 1$; (**a**) free-surface solitary waves excited by FHN pulses for $\mathrm{Ma} = 0-10$ in steps of 1. The arrows point in the direction of increasing Ma; (**b**) corresponding reaction–diffusion pulses for ζ (solid lines) and ξ (dashed lines)

A linear stability analysis of this set of equations reveals that the coupling between the hydrodynamics and reaction–diffusion process has a profound influence on the liquid film. The free surface is linearly stable in the absence of the Marangoni effect but its coupling to the linearly unstable reaction–diffusion system through the Marangoni effect leads to its destabilization. For the parameter values examined here, the instability assumes the form of a spatially periodic cellular pattern.

On the other hand, when the reaction–diffusion process in the absence of convection is linearly stable, in which case there exist traveling waves in the form of fronts or pulses, there also exist traveling waves for the coupled thin-film/excitable medium. Such waves take the form of fronts or pulses for the reaction–diffusion process and pulses for the free surface.

Finally, there are a number of interesting questions related to the analysis presented here. For example, it would be interesting to perform a stability analysis of the traveling waves computed here. Another related problem would be the influence of the kinetic scheme on the type of hydrodynamic interfacial waves triggered by the Marangoni

effect (e.g. a two-variable Oregonator model to describe the kinetics in Belousov–Zhabotinsky systems [44]). These and other problems will be addressed in a future study.

Acknowledgements We acknowledge financial support from the Engineering and Physical Sciences Research Council of England (EPSRC) through grants no. GR/S7912 and no. GR/S01023. SK acknowledges financial support from the EPSRC through an Advanced Research Fellowship, grant no. GR/S49520. UT acknowledges support by the European Union (MRTN-CT-2004–005728).

References

1. Pearson J (1958) On convection cells induced by surface tension. J Fluid Mech 4: 489–500
2. Sternling CV, Scriven LE (1959) Interfacial turbulence: hydrodynamic stability and the Marangoni effect. AIChE J 5: 514–523
3. Bankoff SG (1994) Significant questions in thin liquid-film heat-transfer. J Heat Transf-Trans ASME 116: 10–16
4. Oron A, Davis SH, Bankoff SG (1997) Long-scale evolution of thin liquid films. Rev Mod Phys 69: 931–980
5. Davis SH (1987) Thermocapillary instabilities. Annu Rev Fluid Mech 19: 403–435
6. Joo SW, Davis SH, Bankoff SG (1991) Two-dimensional theory of uniform layers. J Fluid Mech 230: 117–146
7. Oron A, Rosenau P (1992) Formation of patterns induced by thermocapillarity and gravity. J Physique II France 2: 131–146
8. Trevelyan PMJ, Kalliadasis S (2004) Wave dynamics on a thin liquid film falling down a heated wall. J Eng Math 50: 177–208
9. Thiele U, Knobloch E (2004) Thin liquid films on a slightly inclined heated plane. Physica D 190: 213–248
10. Scheid B, Ruyer-Quil C, Thiele U, Kabov OA, Legros JC, Colinet P (2005) Validity domain of the Benney equation including the Marangoni effect for closed and open flows. J Fluid Mech 527: 303–335
11. Ruyer-Quil C, Scheid B, Kalliadasis S, Velarde MG, Zeytounian RKh (2005) Thermocapillary long waves in a liquid film flow. Part 1. Low dimensional formulation. J Fluid Mech 538: 199–222
12. Scheid B, Ruyer-Quil C, Kalliadasis S, Velarde MG, Zeytounian RKh (2005) Thermocapillary long waves in a liquid film flow. Part 2. Linear stability and nonlinear waves. J Fluid Mech 538: 223–244
13. Kalliadasis S, Kiyashko A, Demekhin EA (2003) Marangoni instability of a thin liquid film heated from below by a local heat source. J Fluid Mech 475: 377–408
14. Scheid B, Oron A, Colinet P, Thiele U, Legros JC (2002) Nonlinear evolution of non-uniformly heated falling liquid films. Phys Fluids 14: 4130–4151
15. Skotheim JM, Thiele U, Scheid B (2003) On the instability of a falling film due to localized heating. J Fluid Mech 475: 1–19
16. Burelbach JP, Bankoff SG, Davis SH (1988) Nonlinear instability of evaporating/condensing liquid films. J Fluid Mech 195: 462–494
17. Tan MJ, Bankoff SG, Davis SH (1990) Steady thermocapillary flows of thin liquid layers. I. Theory. Phys Fluids 2: 313–321
18. Burelbach JP, Bankoff SG, Davis SH (1990) Steady thermocapillary flows of thin liquid layers. II. Experiment. Phys Fluids 2: 321–333
19. Bestehorn M, Pototsky A, Thiele U (2003) 3D large scale Marangoni convection in liquid films. Eur Phys J B 33: 457–467
20. De Wit A, Gallez D, Christov CI (1994) Nonlinear evolution equations for thin liquid films with insoluble surfactants. Phys Fluids 6: 3256–3266
21. Schwartz LW, Weidner DE, Eley RR (1995) An analysis of the effect of surfactant on the leveling behavior of a thin liquid coating layer. Langmuir 11: 3690–3693
22. Weidner DE, Schwartz LW, Eley RR (1996) Role of surface tension gradients in correcting coating defects in corners. J Colloid Interface Sci 179: 66–75
23. Matar OK, Troian SM (1999) The development of transient fingering patterns during the spreading of surfactant coated films. Phys Fluids 11: 3232–3246
24. Pismen LM (1984) Composition and flow patterns due to chemo-Marangoni instability in liquid films. J Colloid Interface Sci 102: 237–247
25. Gallez D, De Wit A, Kaufman M (1996) Dynamics of a thin liquid film with surface chemical reaction. J Colloid Interface Sci 180: 524–536
26. Trevelyan PMJ, Kalliadasis S, Merkin JH, Scott SK (2002) Dynamics of a vertically falling film in the presence of a first-order chemical reaction. Phys Fluids 14: 2402–2421
27. Trevelyan PMJ, Kalliadasis S (2004) Dynamics of a reactive falling film at large Péclet numbers. I. Long-wave approximation. Phys Fluids 16: 3191–3208
28. Trevelyan PMJ, Kalliadasis S (2004) Dynamics of a reactive falling film at large Péclet numbers. II. Nonlinear waves far from criticality: Integral-boundary-layer approximation. Phys Fluids 16: 3209–3226
29. Domingues Dos Santos F, Ondarçuhu T (1995) Free-running droplets. Phys Rev Lett 75: 2972–2975
30. Lee SW, Kwok DY, Laibinis PE (2002) Chemical influences on adsorption-mediated self-propelled drop movement. Phys Rev E 65: art. no. 051602-1-9
31. Sumino Y, Nagayama M, Kitahata H, Nomura S-iM, Magome N, Mori Y, Yoshikawa K (2005) Chemo-sensitive running droplet. Phys Rev E 72: art. no. 041603-1-8

32. Thiele U, John K, Bär M (2004) Dynamical model for chemically driven running droplets. Phys Rev Lett 93: art. no. 027802-1-4
33. John K, Bär M, Thiele U (2005) Self-propelled running droplets on solid substrates driven by chemical reactions. Eur Phys J E 18: 183–199
34. Brochard-Wyart F, de Gennes PG (1995) Spontaneous motion of a reactive droplet. C R Acad Sci Ser II 321: 285–288
35. Meron E (1992) Pattern formation in excitable media. Phys Rep 218: 1–66
36. Hagberg AA (1994) Fronts and patterns in reaction-diffusion equations. PhD thesis, University of Arizona
37. Stone HA (1990) A simple derivation of the time-dependent convective diffusion equation for surfactant transport along a deforming interface. Phys Fluids 2: 111–112
38. Williams HAR (1998) Two-dimensional surfactant-driven flows of thin liquid films. PhD thesis, University of Cambridge
39. FitzHugh R (1961) Impulses and physiological states in theoretical models of nerve membrane. Biophys J 1: 445–466
40. Borgas MS, Grotberg JB (1988) Monolayer flow on a thin film. J Fluid Mech 193: 159–170
41. Jensen OE, Grotberg JB (1992) Insoluble surfactant spreading on a thin viscous film: shock evolution and film rupture. J Fluid Mech 240: 259–288
42. Ruckenstein E, Jain RK (1974) Spontaneous rupture of thin liquid films. J Chem Soc Faraday Trans II 70: 132–147
43. Doedel E, Champneys A, Fairfrieve T, Kuznetsov Y, Sandstede B, Wang X (1997) AUTO 97 Continuation and bifurcation software for ordinary differential equations. Montreal Concordia University AUTO 97 and Homcont package for homoclinic orbits continuation are freely distributed and can be found on the web for example at the address: ftp.concordia.ca/pub/doedel/auto
44. Kiss I, Merkin JH, Scott SK, Simon PL (2004) Electric field effects on travelling waves in the Oregonator model for the Belousov-Zhabotinsky reaction. Q J Mech Appl Math 57: 467–494